OPEN ACCESS
IOP Publishing
Journal of Physics A: Mathematical and Theoretical
J. Phys. A: Math. Theor. **57** (2024) 355701 (17pp)
https://doi.org/10.1088/1751-8121/ad6db0

A scalar field theory of 1+1-dimensional laser wakefield accelerators

Mark Aleksiejuk and David A Burton*

Department of Physics, Lancaster University, Lancaster LA1 4YB, United Kingdom

E-mail: d.burton@lancaster.ac.uk

Received 7 December 2023; revised 22 July 2024
Accepted for publication 9 August 2024
Published 20 August 2024

Abstract

A relativistic non-linear scalar field theory is developed from a 2+2-dimensional decomposition of the cold plasma field equations, and the theory is used to investigate a 1+1-dimensional description of a laser wakefield accelerator. The relationship between the properties of a compact laser pulse and its wake is explored. Non-linear solutions are sought describing a regular (i.e. unbroken) wake driven by a prescribed rectangular circularly-polarised laser pulse. An upper bound on the dimensionless amplitude a_0 of the laser pulse is determined as a function of the phase speed v of the wake. The asymptotic behaviour of the upper bound on a_0 as $v \to c$ is shown to agree with well-established, but approximate, results obtained using the conventional encoding of the plasma degrees of freedom. Our approach leads to a closed-form expression for the upper bound on a_0 which is exact for all values of the phase speed of the wake, unlike conventional results that are applicable only when v is sufficiently close to c.

Keywords: laser wakefield acceleration, nonlinear field theory, wave-breaking limit

1. Introduction

The laser wakefield accelerator paradigm has received considerable attention, and undergone significant advancement, since its inception over four decades ago [1]. The essential idea is to accelerate electrons using the very strong electric field of the non-linear wake driven by an ultra-short high intensity laser pulse propagating through an underdense plasma (see [2, 3]

* Author to whom any correspondence should be addressed.

for a review, and [4] for a recent pedagogical overview). The electric field within the wake is approximately three orders of magnitude greater than the electric field achievable within conventional radio-frequency accelerator cavities. Conclusive evidence of the production of high-quality beams of electrons, with energies of order 100 MeV, from laser wakefield accelerators was first reported in 2004 [5–7], and subsequent improvements in laser performance have yielded steady progress. In recent years, high-quality electron beams with multi-GeV energies have been produced within centimeters of plasma [8], and achieving equivalent energies using conventional methods requires accelerator technology that is substantially larger than its laser-plasma-based counterpart. Thus, the laser wakefield acceleration paradigm offers the possibility of compact sources (in comparison to their conventional counterparts) of x-rays and gamma rays for medical, industrial and scientific use [9–12]. Furthermore, it is expected that the middle of the 21st century will see the construction of a laser-plasma-based TeV particle collider. In principle, laser-driven plasma-based accelerators can accelerate leptons to multi-TeV energies over distances of order 1 km, potentially reducing the cost, as well as the size, of future particle colliders [13]. A recent summary of the status of laser wakefield acceleration, and its applications, can be found in [14].

The design of laser wakefield accelerators is underpinned by state-of-the-art three-dimensional particle-in-cell codes, such as OSIRIS [15] and EPOCH [16]. However, such codes require considerable computational resources to use effectively; hence, it is not uncommon to make use of reduced models and scaling arguments [17, 18] in the first instance. One-dimensional models and analytical results remain useful for making preliminary estimates [19, 20], especially when exploring the implications of new physics [21]. Furthermore, it is conceivable that alternative encodings of the laser-plasma degrees of freedom may yield useful insights that do not readily emerge from conventional approaches.

The purpose of this article is to explore the implications of a relativistically covariant nonlinear scalar field theory that naturally emerges from a particular exact reduction of the coupled field system describing a laser-driven plasma. As far as we are aware, the scalar field equation that encodes the plasma electron degrees of freedom has not been used previously in the context of laser wakefield accelerators. In addition to yielding the same results as conventional methods [19], we show that our framework also leads to the relationship

$$a_0^2 \leqslant \frac{c^2\,(\gamma-1)}{4v^2}\left(\frac{v^4}{c^4}+\frac{6v^2}{c^2}+1-\frac{1}{\gamma^3}\right) \tag{1}$$

between the dimensionless amplitude a_0 of a circularly polarised rectangular laser pulse and the phase speed v of its wake. The laser pulse and plasma wake both propagate rectilinearly at the subluminal speed v, and thus have Lorentz factor $\gamma = 1/\sqrt{1-v^2/c^2}$ where c is the vacuum speed of light.

If the bound in (1) is not satisfied then the wake breaks. From a general perspective, the onset of wave-breaking is an important concept in laser wakefield acceleration because it is accompanied by a build-up of trapped plasma electrons, which are subsequently accelerated by the electric field of the wake. A good understanding of wave-breaking is important for controlling the properties of the electron bunches that emerge from this process [22].

It is notable that the upper bound on the dimensionless amplitude a_0 given in (1) agrees with the quantity $\sqrt{2(\gamma-1)}$ to within 3.2% accuracy over the entire range $0 < v < c$. The amplitude of the electric field of the strongest possible periodic wake is $m\omega_p c\sqrt{2(\gamma-1)}/e$, where m is the electron mass, e is the elementary charge and ω_p is the plasma angular frequency. Moreover, the amplitude of the electric field of the laser pulse is given by $m\omega_0 c\,a_0/e$ where ω_0 is the angular frequency of the laser pulse. Hence, the ratio of the upper bounds on the

amplitudes of the electric fields of the laser pulse and the plasma wake is almost equal to ω_0/ω_p throughout $0 < v < c$. The ratio of the upper bounds tends to unity as $v \to c$.

The relationship between the dimensionless amplitude of the laser pulse and the amplitude of the electric field of the wake is usually explored in a regime where v is close to c [2, 19]. Approximations adapted to this regime are often introduced from the outset, greatly simplifying the subsequent analysis. The asymptotic behaviour $a_0^2 \lesssim 2\gamma$, as $v \to c$, of our new result (1) coincides with the results of those approximations [2, 19]. However, the approach we take naturally yields a result that is accurate for all v throughout the range $0 < v < c$, not only when v is sufficiently close to c. We will explore this comparison in more detail in section 3.4.

Henceforth, we use units in which the permittivity of the vacuum satisfies $\varepsilon_0 = 1$ and the speed of light satisfies $c = 1$.

2. Field equations

For simplicity, we focus on the behaviour of non-linear laser-driven plasma waves in a regime where the temperature of the electrons and the motion of the ions can be neglected. It is sufficient in this regime to make use of 'cold' fluid models of both particle species. As we will now show, a scalar field theory naturally emerges when the physical variables are represented in terms of exterior differential forms[1]. Exterior differential calculus is well-suited to the analysis of relativistically covariant field systems, such as Maxwell's equations, as the nilpotency of the exterior derivative is particularly useful in this context. See [23] for an introduction to exterior differential calculus in terms of the conventions used here.

The Gauss–Ampère law and Gauss–Faraday law can be expressed as

$$d \star F = -qn \star \widetilde{V} + qn_{\text{ion}} \star \widetilde{V}_{\text{ion}}, \tag{2}$$

$$dF = 0 \tag{3}$$

where F is the electromagnetic 2-form, V is the four-velocity of the electron fluid, V_{ion} is the four-velocity of the ion fluid, n is the proper number density[2] of the electron fluid, n_{ion} is the proper number density of the ion fluid, and $q = -e$ is the charge on an electron. In turn, the electron fluid is driven by the Lorentz force. Thus, V satisfies the relativistic version

$$m\iota_V d\widetilde{V} = q\widetilde{\iota_V F} \tag{4}$$

of Newton's second law[3], where ι_X denotes the interior product with respect to the vector field X and the tilde denotes the metric dual operation (i.e. $\widetilde{X} = g(X, -)$ and $\widetilde{\alpha} = g^{-1}(\alpha, -)$ where α is a 1-form and g is the spacetime metric, with g^{-1} its inverse). The Hodge map is denoted $\star$, d is the exterior derivative and the metric signature $+2$ (i.e. the pattern $-+++$ of signs) is used. Hence, the four-velocities are normalised as

$$g(V, V) = -1, \qquad g(V_{\text{ion}}, V_{\text{ion}}) = -1. \tag{5}$$

[1] The scalar field theory is given explicitly in terms of partial derivatives in (27)–(29) for readers unfamiliar with the calculus of differential forms.

[2] The proper number density of a fluid is the number density measured by an observer co-moving with the fluid. The number density in the laboratory frame is the proper number density multiplied by the Lorentz factor of the velocity of the fluid in the laboratory frame.

[3] The left-hand side of (4) is a rewriting of the rate of change of four-momentum with respect to the proper time of the plasma electrons. The result $\nabla_V \widetilde{P} = m\iota_V d\widetilde{V}$, where ∇ is the Levi–Civita connection and $P = mV$ is the four-momentum of the plasma electrons, follows from the identity $\nabla_X \widetilde{X} = \iota_X d\widetilde{X} + \frac{1}{2} d[g(X, X)]$ and the fact $g(V, V)$ is constant.

2.1. 2+2-dimensional decomposition

Let $\{t,x,y,z\}$ be Minkowski coordinates in the laboratory frame. Introduction of the Minkowski metric

$$g = -dt \otimes dt + dx \otimes dx + dy \otimes dy + dz \otimes dz \tag{6}$$

and the volume 4-form $\star 1 = dt \wedge dx \wedge dy \wedge dz$ allows the field equations (2)–(5) to be readily decomposed into (t,z) and (x,y) subspaces. From the outset, we focus on solutions to the field equations whose components with respect to the coordinate frame $\{\partial/\partial t, \partial/\partial x, \partial/\partial y, \partial/\partial z\}$ only depend on (t,z).

2.1.1. Decomposition of Maxwell's equations. The electromagnetic 2-form F can be expressed as:

$$F = E\#_{\parallel}1 + dA_j \wedge dx^j - B\#_{\perp}1, \tag{7}$$

where the Hodge maps $\#_{\parallel}$ and $\#_{\perp}$ are induced from the volume 2-forms $\#_{\parallel}1 = dt \wedge dz$ and $\#_{\perp}1 = dx \wedge dy$, respectively. E and B are 0-forms, while $A_j dx^j$ is a 1-form[4], with $j = 1,2$ corresponding to the x and y components respectively. As noted previously, we require E, B, A_1 and A_2 to only depend on (t,z); thus, for example, $dA_j \in \mathrm{span}\{dt, dz\}$. Inspection of (7) shows $\{E_x = \partial A_1/\partial t, E_y = \partial A_2/\partial t, E_z = E\}$ are the components of the electric field and $\{B_x = \partial A_2/\partial z, B_y = -\partial A_1/\partial z, B_z = B\}$ are the components of the magnetic field according to observers with four-velocity $\partial/\partial t$. Likewise, the four-velocity field V is decomposed as

$$V = V_{\parallel} + V_{\perp} \tag{8}$$

where $V_{\parallel} \in \mathrm{span}\{\partial/\partial t, \partial/\partial z\}$ and $V_{\perp} \in \mathrm{span}\{\partial/\partial x, \partial/\partial y\}$. Furthermore, we require $V_{\mathrm{ion}} \in \{\partial/\partial t, \partial/\partial z\}$.

Introducing (7) into the Gauss–Faraday law (3) reveals B is constant, while the Gauss–Ampère law (2) yields

$$dE = qn\#_{\parallel}\widetilde{V}_{\parallel} - qn_{\mathrm{ion}}\#_{\parallel}\widetilde{V}_{\mathrm{ion}}, \tag{9}$$

$$d\#_{\parallel}dA_j = qnV_j\#_{\parallel}1 \tag{10}$$

where, in addition to (7), the decomposition (8) has been used and $\{V_1, V_2\}$ are the components of $\widetilde{V}_{\perp} = V_j dx^j$.

Every closed differential form (i.e. a differential form α that satisfies $d\alpha = 0$) can be locally expressed as an exact differential form (i.e. $\alpha = d\beta$); see the converse of the Poincaré lemma in, for example, [24]. The electron fluid number current and ion fluid number current are independently conserved, and thus the 1-forms $n\#_{\parallel}\widetilde{V}_{\parallel}$ and $n_{\mathrm{ion}}\#_{\parallel}\widetilde{V}_{\mathrm{ion}}$ are each closed. Hence, we can introduce 0-forms N and N_{ion} satisfying

$$dN = n\#_{\parallel}\widetilde{V}_{\parallel}, \tag{11}$$

$$dN_{\mathrm{ion}} = n_{\mathrm{ion}}\#_{\parallel}\widetilde{V}_{\mathrm{ion}} \tag{12}$$

[4] The Einstein summation convention is used.

which, when combined with (9), yield the expression

$$E = q\,(N - N_{\text{ion}}) \tag{13}$$

up to an integration constant. Each point (t, z) corresponds to a 2-dimensional spacelike slice of 4-dimensional spacetime, and the absolute value of N (N_{ion}) is the total number of plasma electrons (ions) per unit area between the slice containing the field point and a fiducial slice. The fiducial slice should be located in a spacetime region where the plasma is in equilibrium, i.e. $nV = n_{\text{ion}} V_{\text{ion}}$. The integration constant omitted from (13) is then the z-component of the electric field due to sources outside the plasma, so it is zero for our purposes.

Equation (13) is a familiar ingredient in conventional studies of non-linear plasma waves when Lagrangian variables are used (see, for example, [25], where an equivalent expression is inferred using physical reasoning). A recent extensive analysis of laser-driven plasma waves using Lagrangian variables can be found in [26]. However, our approach to the quantities N and N_{ion} (and, as a consequence, E) is geometrical. It does not require coordinates (Lagrangian or otherwise); instead, the results follow immediately from charge conservation and the converse of the Poincaré lemma (i.e. the fact that every closed differential form is locally exact).

2.1.2. Decomposition of the relativistic version of Newton's second law. Introducing (7) and (8) into (4) leads to

$$\iota_{V_\parallel} d\widetilde{V}_\parallel - V^j dV_j = \frac{q}{m}\left(E\#_\parallel \widetilde{V}_\parallel - V^j dA_j\right), \tag{14}$$

$$\left(\iota_{V_\parallel} dV_j\right) dx^j = \frac{q}{m}\left(\iota_{V_\parallel} dA_j\right) dx^j - \frac{q}{m} B\#_\perp \widetilde{V}_\perp \tag{15}$$

where $\{V^1, V^2\}$ are the components of $V_\perp = V^j \partial_j$ with $\partial_1 = \partial/\partial x$ and $\partial_2 = \partial/\partial y$. Note $V_j = \delta_{jk} V^k$, where δ_{jk} is the Kronecker delta, because of the structure of the metric.

We previously noted that the Gauss–Faraday law ensures the z-component B of the magnetic field is constant; thus, it must be induced by currents outside the plasma. Our focus here is on unmagnetised plasma, so we set $B = 0$. Hence, (14) can be reduced further to

$$\iota_{V_\parallel} d\widetilde{V}_\parallel = \frac{q}{m} E\#_\parallel \widetilde{V}_\parallel \tag{16}$$

by introducing the solution

$$V_j = \frac{q}{m} A_j \tag{17}$$

to (15). Furthermore, $d\widetilde{V}_\parallel$ is a top-dimensional form on a 2-dimensional spacetime, and it follows (16) is satisfied if and only if[5]

$$d\widetilde{V}_\parallel = \frac{q}{m} E\#_\parallel 1. \tag{18}$$

[5] Clearly, (18) immediately implies (16) because $\iota_X \#_\parallel 1 = \#_\parallel \widetilde{X}$ for all $X \in \text{span}\{\partial/\partial t, \partial/\partial z\}$. One can show (16) yields (18) by noting $\alpha \wedge d\widetilde{V}_\parallel = 0$ for all $\alpha \in \text{span}\{dt, dz\}$ and substituting (16) in the expansion of $\iota_{V_\parallel}(\alpha \wedge d\widetilde{V}_\parallel) = 0$.

2.1.3. Emergence of a scalar field theory. To proceed further, it is fruitful to make use of (11) and the proper-time normalisation condition (5) on V to eliminate $\widetilde{V}_{\parallel}$, $\widetilde{V}_{\perp}$ and n in favour of N. We begin by noting $\#_{\parallel}\#_{\parallel} = 1$ on 1-forms in the span of $\{dt, dz\}$, and so

$$\widetilde{V}_{\parallel} = \left\|\widetilde{V}_{\parallel}\right\| \frac{\#_{\parallel} dN}{\left\|\#_{\parallel} dN\right\|} \tag{19}$$

follows from (11). The vertical brackets $\|\ldots\|$ denote the norm on 1-forms induced by the metric, i.e.

$$\|\beta\| = \sqrt{|g^{-1}(\beta,\beta)|} \tag{20}$$

where β is a 1-form. The inner product $g^{-1}(\#_{\parallel} dN, \#_{\parallel} dN)$ can be shown to satisfy

$$g^{-1}\left(\#_{\parallel} dN, \#_{\parallel} dN\right) = -g^{-1}\left(dN, dN\right), \tag{21}$$

which implies $\left\|\#_{\parallel} dN\right\| = \|dN\|$. Furthermore,

$$\begin{aligned} g(V,V) &= -\left\|\widetilde{V}_{\parallel}\right\|^2 + \left\|\widetilde{V}_{\perp}\right\|^2 \\ &= -\left\|\widetilde{V}_{\parallel}\right\|^2 + |\mathcal{A}|^2 \end{aligned} \tag{22}$$

where, using (17), $\left\|\widetilde{V}_{\perp}\right\|$ has been substituted by the magnitude of the complex scalar field $\mathcal{A} = \frac{q}{m}(A_1 + iA_2)$. Hence, using $g(V,V) = -1$, we find

$$\left\|\widetilde{V}_{\parallel}\right\| = \sqrt{1 + |\mathcal{A}|^2}, \tag{23}$$

and so, using (13) to eliminate the z-component E of the electric field and (19) to eliminate $\widetilde{V}_{\parallel}$, the remnant (18) of the relativistic version of Newton's second law can be expressed as

$$d\left(\sqrt{1 + |\mathcal{A}|^2}\frac{\#_{\parallel} dN}{\|dN\|}\right) = \frac{q^2}{m}\left(N - N_{\text{ion}}\right)\#_{\parallel} 1. \tag{24}$$

Furthermore, using (11) and (23), the proper number density n can be expressed as

$$n = \frac{\|dN\|}{\sqrt{1 + |\mathcal{A}|^2}}, \tag{25}$$

which, using (17), immediately allows (10) to be written as

$$d\#_{\parallel} d\mathcal{A} = \frac{q^2}{m}\frac{\|dN\|}{\sqrt{1 + |\mathcal{A}|^2}}\mathcal{A}\#_{\parallel} 1. \tag{26}$$

Decomposing (24) and (26) in terms of the coordinate frame $\{\partial/\partial t, \partial/\partial z\}$ yields

$$\frac{\partial}{\partial t}\left(\frac{\sqrt{1+|\mathcal{A}|^2}}{\|dN\|}\frac{\partial N}{\partial t}\right) - \frac{\partial}{\partial z}\left(\frac{\sqrt{1+|\mathcal{A}|^2}}{\|dN\|}\frac{\partial N}{\partial z}\right) = -\frac{q^2}{m}\left(N - N_{\text{ion}}\right), \tag{27}$$

$$\frac{\partial^2 \mathcal{A}}{\partial t^2} - \frac{\partial^2 \mathcal{A}}{\partial z^2} = -\frac{q^2}{m}\frac{\|dN\|}{\sqrt{1+|\mathcal{A}|^2}}\mathcal{A} \tag{28}$$

where

$$\|dN\| = \sqrt{\left(\frac{\partial N}{\partial z}\right)^2 - \left(\frac{\partial N}{\partial t}\right)^2}. \tag{29}$$

The relative sign of the two terms within the square root in (29) follows from (20) because dN is spacelike. The results $\#_{\|} dt = -dz$ and $\#_{\|} dz = -dt$, which follow from $\#_{\|}\widetilde{X} = \iota_X \#_{\|} 1$ and $\#_{\|} 1 = dt \wedge dz$, have been used to obtain (27) and (28).

Furthermore, the components of (11) are

$$\frac{\partial N}{\partial z} = n\Gamma, \qquad \frac{\partial N}{\partial t} = -n\Gamma u \tag{30}$$

where $\Gamma = dt(V_{\|})$ is the Lorentz factor of the plasma electrons and $u = dz(V_{\|})/\Gamma$ is the z-component of their three-velocity in the laboratory frame. Note $n\Gamma$ is the number density of the plasma electrons in the laboratory frame. Likewise, inspection of (12) shows that

$$\frac{\partial N_{\text{ion}}}{\partial z} = n_{\text{ion}}\Gamma_{\text{ion}}, \qquad \frac{\partial N_{\text{ion}}}{\partial t} = -n_{\text{ion}}\Gamma_{\text{ion}}u_{\text{ion}} \tag{31}$$

are satisfied by the Lorentz factor $\Gamma_{\text{ion}} = dt(V_{\text{ion}})$, three-velocity z-component $u_{\text{ion}} = dz(V_{\text{ion}})/\Gamma_{\text{ion}}$ and number density $n_{\text{ion}}\Gamma_{\text{ion}}$ of the plasma ions in the laboratory frame. See [27] for a derivation of (30) and (31) using Lagrangian variables.

Given appropriate boundary conditions, and the details of the 0-form N_{ion}, we see that (24) and (26) provide a closed system of second-order partial differential equations for the scalar fields N and $\mathcal{A}$.

3. Plasma wave driven by a circularly polarised laser pulse

Although (24) and (26) are concise, they comprise a fully-coupled system of non-linear partial differential equations and do not readily yield exact analytical solutions describing the multi-scale interaction of a laser pulse and a plasma. However, progress can be made if, following one of the strategies adopted in [19], we forego (26) in favour of prescribing $|\mathcal{A}|$ as data and focus exclusively on the field equation (24) for N. This approach neglects, for example, the depletion of the laser pulse as it propagates through the plasma [19]. Our focus is on properties of the system whose time scales are much shorter than those of the energy loss of the laser pulse. Furthermore, over such timescales, we regard the ions as static and to have constant density; thus, we satisfy (12) by introducing $V_{\text{ion}} = \partial/\partial t$ and $N_{\text{ion}} = n_{\text{ion}} z$.

Our analysis of the oscillatory wake driven by the laser pulse begins by adopting the 'quasi-static' approximation in which the dimensionless envelope $a = |\mathcal{A}|$ of the laser pulse and the areal number density $N - N_{\text{ion}}$ are functions of the variable $\zeta = z - vt$ only. The constant v

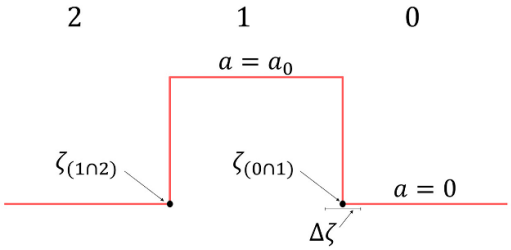

Figure 1. The structure of $a(\zeta)$ for a laser pulse with a top-hat envelope (shown in red). The pulse is travelling from left to right. The domain of a is separated into region 0 in front of the travelling pulse, region 1 within the pulse and region 2 occupied by the plasma wake. Parentheses surround labels when they refer to the regions and their intersections, to avoid confusion with, for example, the subscript on the conventional symbol a_0 for the dimensionless laser amplitude in laser-plasma physics. The subscript $(0\cap1)$ indicates the front of the pulse, while the subscript $(1\cap2)$ indicates the back of the pulse.

is the phase speed of the wake and the speed of the envelope of the laser pulse[6] and satisfies $0 < v < 1$. The laser pulse propagates subluminally in the direction of increasing z, at the same speed v as its wake, in the rest frame of the ions. The behaviour of the internal oscillations of the laser pulse are determined by the argument of the complex 0-form $\mathcal{A}$ and have much higher frequency than the wake. They do not play a role in the following analysis.

It is convenient to introduce the substitution $N = n_{\text{ion}}\psi + n_{\text{ion}}z$ to the field equation (24), where ψ is a function of ζ only. Equation (24) then reduces to

$$\left(\sqrt{1+a^2}\,\frac{1+\psi'-v^2\psi'}{\sqrt{(1+\psi')^2-v^2\psi'^2}}\right)' = \omega_p^2\psi. \tag{32}$$

where the plasma angular frequency satisfies $\omega_p = \sqrt{q^2 n_{\text{ion}}/m}$ and a prime denotes differentiation with respect to ζ. The properties of analytical solutions to (32) when the envelope of the laser pulse is a piecewise constant function of ζ can be readily obtained. Figure 1 shows a simple model of the envelope of a circularly polarised laser pulse in which $a = a_0$ throughout the pulse, and $a = 0$ outside the pulse. The behaviour of ψ in this case is well-approximated by direct numerical integration of (32) with the smooth envelope

$$a(\zeta) = \frac{a_0}{4}\left[1+\tanh\left(\frac{\zeta-\sigma+w}{s}\right)\right]\left[1+\tanh\left(\frac{-\zeta+\sigma+w}{s}\right)\right], \tag{33}$$

where the parameters σ, w and s control the location of the centre of the pulse, the duration of the pulse and the 'steepness' of the edges of the pulse. Numerical solutions to (32) are graphed in figure 2, alongside analytical results we will soon derive using the top-hat expression for $a(\zeta)$.

[6] The simplest way to quantify v in terms of the laser and plasma properties is to identify it with the group speed of the laser pulse in the linear 1D regime (see, for example, [2, 19]). This approach yields the expression $\gamma = \omega_0/\omega_p$ for the Lorentz factor of v, where ω_0 is the angular frequency of the laser and ω_p is the plasma angular frequency. The expression $\gamma = \omega_0/\omega_p$ can be obtained by linearising (26) in $\mathcal{A}$ when $N = N_{\text{ion}} = n_{\text{ion}}z$, although the use of this approximation is questionable when the laser pulse is sufficiently strong. Expressions for γ valid outside of the linear 1D regime can be found in [2].

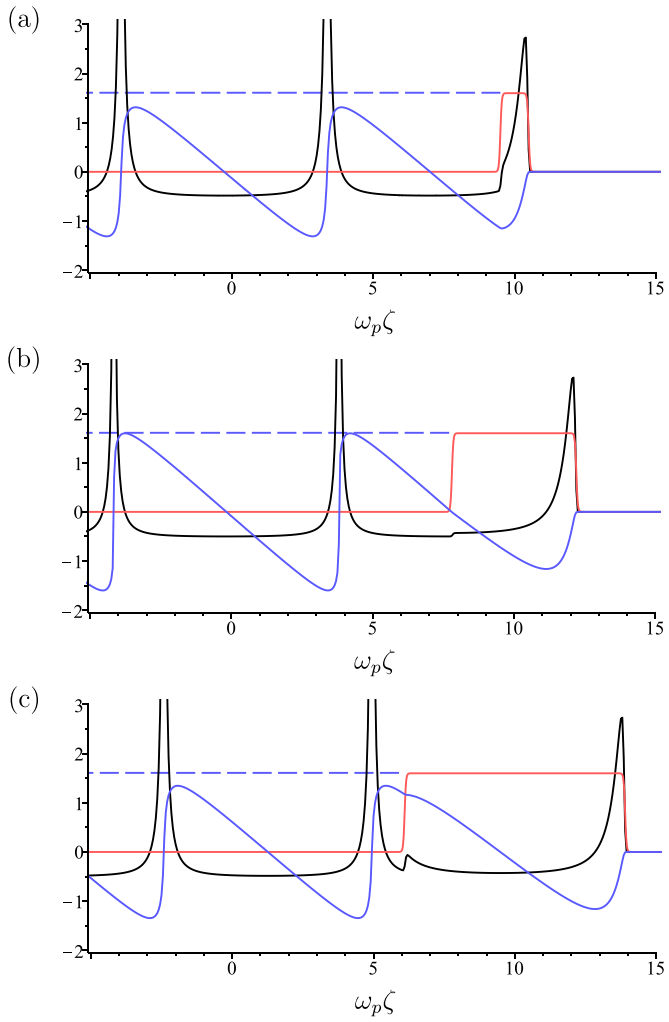

Figure 2. Numerical solutions to (32) corresponding to a laser pulse with dimensionless envelope (33) and dimensionless amplitude $a_0 = 1.6$. The envelope of the laser pulse has centre $\sigma = 10/\omega_p$, 'steepness' $s = 0.05/\omega_p$ and duration $2\omega_p w \in \{1.0, 4.4, 7.8\}$. The speed of the wake is $v = 0.9$. The dimensionless envelope of the laser pulse is shown in red. The quantity $\omega_p\psi$ is shown in blue, while ψ' is shown in black. The blue dotted line shows the maximum value $\sqrt{2(\gamma-1)}$ of $\omega_p\psi$ for the largest amplitude oscillatory solution to (32) behind the pulse. The maxima of ψ' behind the pulse have been cropped for convenience. The numerical value of a_0 is marginally below its maximum $a_{0c} = 1.603$ (3 decimal places) given by (49).

Figure 2 demonstrates the well-established result that the strongest wake is generated by a pulse whose envelope occupies one-half of the first oscillation of the electric field [2, 19]. Such pulses are said to have *optimal length*, and we will focus on optimal-length pulses throughout the following analysis. Pulses whose shape is different from (33) have different optimal lengths [2].

3.1. Across the front of the laser pulse

Our first step is to use (32) to derive a jump condition on ψ' across the front of the pulse. Since ψ is bounded, integrating (32) over a small interval in ζ centred at the front $\zeta = \zeta_{(0\cap1)}$ of the pulse, and letting the size $\Delta\zeta$ of the interval tend to zero, yields

$$\lim_{\Delta\zeta\to0}\left[\sqrt{1+a^2}\,\frac{1+\psi'-v^2\psi'}{\sqrt{(1+\psi')^2-v^2\psi'^2}}\right]_{\zeta_{(0\cap1)}-\Delta\zeta/2}^{\zeta_{(0\cap1)}+\Delta\zeta/2}=0. \tag{34}$$

The laser pulse envelope is such that $a=0$ outside the pulse and $a=a_0$ inside the pulse. The plasma is in equilibrium throughout region 0 ahead of the pulse (i.e. $\psi_{(0)}=0$), so $\psi'^{+}_{(0\cap1)}=0$. Equation (34) reduces to

$$1-\sqrt{1+a_0^2}\,\frac{1+\psi'^{-}_{(0\cap1)}-v^2\psi'^{-}_{(0\cap1)}}{\sqrt{\left(1+\psi'^{-}_{(0\cap1)}\right)^2-v^2\psi'^{-2}_{(0\cap1)}}}=0, \tag{35}$$

where the $+/-$ superscript denotes the limit of a function at a boundary (in this case, $0\cap1$) approached from ahead/behind respectively, i.e. $f^{\pm}_{(0\cap1)}=\lim_{\Delta\zeta\to0}f(\zeta_{(0\cap1)}\pm\Delta\zeta/2)$.

3.2. Inside the laser pulse

Equation (32) is the Euler–Lagrange equation of

$$L=-\sqrt{1+a^2}\sqrt{(1+\psi')^2-v^2\psi'^2}+\sqrt{1+a^2}-\frac{1}{2}\omega_p^2\psi^2 \tag{36}$$

where, for convenience, $L=0$ is chosen to coincide with ψ being identically zero. Inside the pulse, where $\psi=\psi_{(1)}$, the Lagrangian

$$L_{(1)}=-\sqrt{1+a_0^2}\sqrt{\left(1+\psi'_{(1)}\right)^2-v^2\psi'^2_{(1)}}+\sqrt{1+a_0^2}-\frac{1}{2}\omega_p^2\psi^2_{(1)} \tag{37}$$

does not explicitly depend on ζ. Therefore, the quantity $\mathcal{E}_{(1)}$ given by

$$\begin{aligned}\mathcal{E}_{(1)}&=\psi'_{(1)}\frac{\partial L_{(1)}}{\partial\psi'_{(1)}}-L_{(1)}\\&=\frac{\sqrt{1+a_0^2}\left(1+\psi'_{(1)}\right)}{\sqrt{\left(1+\psi'_{(1)}\right)^2-v^2\psi'^2_{(1)}}}-\sqrt{1+a_0^2}+\frac{1}{2}\omega_p^2\psi^2_{(1)}\end{aligned} \tag{38}$$

is constant.

Although the derivative of ψ jumps across the front of the pulse, ψ itself is continuous. Since ψ vanishes ahead of the pulse (region 0), we have $\psi^{+}_{(0\cap1)}=0$; hence, $\psi^{-}_{(0\cap1)}=0$. Therefore, evaluating (38) in the limit as ζ tends to $\zeta_{(0\cap1)}$ from below gives

$$\mathcal{E}_{(1)} = \frac{\sqrt{1+a_0^2}\left(1+\psi'^{-}_{(0\cap 1)}\right)}{\sqrt{\left(1+\psi'^{-}_{(0\cap 1)}\right)^2 - v^2\psi'^{-2}_{(0\cap 1)}}} - \sqrt{1+a_0^2}. \tag{39}$$

Equation (35) has two solutions for $\psi'^{-}_{(0\cap 1)}$. Only one of the solutions,

$$\psi'^{-}_{(0\cap 1)} = \gamma^2\left(-1+\frac{\gamma v}{\sqrt{\gamma^2-1-a_0^2}}\right), \tag{40}$$

is physically admissible because it vanishes when $a_0 = 0$ (i.e. when there is no laser pulse to drive the plasma away from equilibrium)[7]. Substituting (40) in (39) yields the expression

$$\mathcal{E}_{(1)} = -\gamma v\sqrt{\gamma^2-1-a_0^2} + \gamma^2 - \sqrt{1+a_0^2} \tag{41}$$

in terms of the speed v and the dimensionless amplitude a_0 of the laser pulse.

Evaluating (38) at a turning point of $\psi_{(1)}$ gives

$$\mathcal{E}_{(1)} = \frac{1}{2}\omega_p^2\psi_{(1)0}^2, \tag{42}$$

where $\psi_{(1)0}$ is the value of $\psi_{(1)}$ at the turning point. However, $N - N_{\text{ion}} = n_{\text{ion}}\psi$ and so, using (13), it follows $E = qn_{\text{ion}}\psi$. Thus, by equating the right-hand sides of (41) and (42), we see that the magnitude of the electric field $E_{(1)} = qn_{\text{ion}}\psi_{(1)}$ inside the laser pulse cannot exceed $|E_{(1)\max}|$ where

$$|E_{(1)\max}| = \frac{m\omega_p}{|q|}\left[2\left(\gamma^2 - \gamma v\sqrt{\gamma^2-1-a_0^2} - \sqrt{1+a_0^2}\right)\right]^{\frac{1}{2}}. \tag{43}$$

The result (43) was obtained in [19] using a different approach.

Inspection of the argument of the innermost square root in (43) reveals the upper bound $a_0 < \gamma v$. However, as we will describe in the next section, not all values of a_0 below γv yield a regular wake behind the pulse, i.e. an oscillatory $\psi_{(2)}$.

3.3. *Through the back of the laser pulse*

We now turn our attention to the behaviour of ψ behind the pulse. Integrating equation (32) across the back of the pulse, and following the approach used to obtain (35), yields the jump condition

$$\frac{1+\psi'^{-}_{(1\cap 2)} - v^2\psi'^{-}_{(1\cap 2)}}{\sqrt{\left(1+\psi'^{-}_{(1\cap 2)}\right)^2 - v^2\psi'^{-2}_{(1\cap 2)}}} - \sqrt{1+a_0^2}\,\frac{1+\psi'^{+}_{(1\cap 2)} - v^2\psi'^{+}_{(1\cap 2)}}{\sqrt{\left(1+\psi'^{+}_{(1\cap 2)}\right)^2 - v^2\psi'^{+2}_{(1\cap 2)}}} = 0 \tag{44}$$

[7] Note $\gamma v = \sqrt{\gamma^2-1}$ because $\gamma = 1/\sqrt{1-v^2}$.

on the values of ψ' on either side of the back $1\cap 2$ of the pulse. Furthermore, following the approach used to obtain (38), we see that the quantity

$$\mathcal{E}_{(2)} = \frac{1+\psi'_{(2)}}{\sqrt{\left(1+\psi'_{(2)}\right)^2 - v^2\psi'^2_{(2)}}} - 1 + \frac{1}{2}\omega_p^2\psi^2_{(2)} \tag{45}$$

is constant at all points behind the pulse (i.e. throughout region 2).

The wake $\psi_{(2)}$ of the pulse is oscillatory if the dimensionless amplitude a_0 of the laser pulse is not too large. A regular wake cannot be sustained if the pulse is too strong; instead, the wake 'breaks' and the simplest cold fluid model, in which there is only one electron fluid component, is no longer applicable. The behaviour of $\psi_{(2)}$ in the limiting case resembles a smoothed sawtooth; see figure 2(b). The strongest wake arises if there exists a point at which $\psi'_{(2)} \to \infty$ as $\psi_{(2)} \to 0$; hence, using (45),

$$\mathcal{E}_{(2)} = \gamma - 1 \tag{46}$$

follows in this case. The amplitude $\sqrt{2(\gamma-1)}/\omega_p$ of $\psi_{(2)}$, obtained by evaluating (45) at a turning point of $\psi_{(2)}$, is shown in figure 2.

For an optimal-length pulse (see figure 2(b)), the field ψ passes through zero at the back of the pulse; hence, $\psi^-_{(1\cap2)} = 0$. Substituting $\psi^-_{(1\cap2)} = 0$ in (45) and eliminating $\mathcal{E}_{(2)}$ using (46) yields $\psi'^-_{(1\cap2)} = -1/2$. Hence, (44) can be expressed as

$$\frac{1+v^2}{\sqrt{1-v^2}} - \sqrt{1+a_{0c}^2}\,\frac{1+\psi'^+_{(1\cap2)} - v^2\psi'^+_{(1\cap2)}}{\sqrt{\left(1+\psi'^+_{(1\cap2)}\right)^2 - v^2\psi'^{+2}_{(1\cap2)}}} = 0 \tag{47}$$

where a_{0c} denotes the critical value of a_0 corresponding to the strongest wake.

However, we also have the equation

$$\gamma^2 - \gamma v\sqrt{\gamma^2 - 1 - a_{0c}^2} - \frac{\sqrt{1+a_{0c}^2}\left(1+\psi'^+_{(1\cap2)}\right)}{\sqrt{\left(1+\psi'^+_{(1\cap2)}\right)^2 - v^2\psi'^{+2}_{(1\cap2)}}} = 0 \tag{48}$$

obtained by combining (38) and (41) after setting $a_0 = a_{0c}$. Solving (47) and (48) simultaneously for $\psi'^+_{(1\cap2)}$ leads to the expression

$$a_{0c}^2 = \frac{\gamma-1}{4v^2}\left(v^4 + 6v^2 + 1 - \gamma^{-3}\right) \tag{49}$$

for the square of the critical dimensionless laser amplitude a_{0c} as a function of the speed v. Although one can obtain this result directly (see appendix), it is worth describing a more nuanced approach informed by the numerical results shown in figure 2(b).

Inspection of the pair of solutions to (48) for $\psi'^+_{(1\cap2)}$, and the properties of ψ' shown in figure 2(b), suggests

$$\psi'^+_{(1\cap2)} = -\frac{\sqrt{\eta^2 - 1 - a_{0c}^2}}{\sqrt{\eta^2 - 1 - a_{0c}^2} + v\eta} \tag{50}$$

is the appropriate choice. The quantity

$$\eta = \gamma^2 - \gamma v\sqrt{\gamma^2 - 1 - a_{0c}^2} \tag{51}$$

has been introduced for convenience. The second solution to (48) is identical to (50) except the denominator is $\sqrt{\eta^2 - 1 - a_{0c}^2} - v\eta$ instead of $\sqrt{\eta^2 - 1 - a_{0c}^2} + v\eta$. Figure 2(b) shows $\psi'^{+}_{(1\cap 2)} \approx \psi'^{-}_{(1\cap 2)} = -1/2$, so inspection of (50) reveals $\sqrt{\eta^2 - 1 - a_{0c}^2}$ must be approximately equal to $v\eta$ (since $\sqrt{\eta^2 - 1 - a_{0c}^2}$ and $v\eta$ are both positive). The magnitude of the second solution to (48) must be somewhat larger than $1/2$; therefore, we reject it.

Comparison of (47) and (48) reveals $\psi'^{+}_{(1\cap 2)}$ must satisfy

$$\frac{\gamma^3\left(1+v^2\right)}{\gamma^2 + \psi'^{+}_{(1\cap 2)}} = \frac{\eta}{1 + \psi'^{+}_{(1\cap 2)}} \tag{52}$$

which, when combined with (50), yields an equation for η whose non-zero solutions satisfy

$$\eta_{\pm} = \gamma^3\left(1+v^2\right) \pm \gamma v\sqrt{\gamma^4\left(1+v^2\right)^2 - 1 - a_{0c}^2}. \tag{53}$$

Hence, (51) and (53) together imply

$$\gamma^2\left(1+v^2\right) - \gamma = \mp v\sqrt{\gamma^4\left(1+v^2\right)^2 - 1 - a_{0c}^2} - v\sqrt{\gamma^2 - 1 - a_{0c}^2} \tag{54}$$

where the minus sign corresponds to η_+ and the plus sign corresponds to η_-. Since $\gamma^2(1+v^2) > \gamma$, we see that the plus sign in (54) is the appropriate choice. Rearranging the resulting expression for a_{0c}^2 yields (49).

3.4. Comparison with the standard methodology

The quantity $a_{0c}/\sqrt{2(\gamma-1)}$, with a_{0c} given by (49), is a monotonically increasing function of v in the range $0 < v < 1$. It tends to $\sqrt{15}/4 = 0.968$ (3 decimal places) as $v \to 0$, and tends to 1 as $v \to 1$. Clearly, $2(\gamma-1)$ is an excellent approximation to (49) throughout the range $0 < v < 1$.

It is illuminating to compare the above to the results of conventional methods [2, 19]. The standard approach is based on the use of a dimensionless potential φ that satisfies the ordinary differential equation

$$\varphi'' = \omega_p^2 v\gamma^2\left(\frac{1+\varphi}{\sqrt{(1+\varphi)^2 - (1+a^2)\gamma^{-2}}} - \frac{1}{v}\right) \tag{55}$$

where the z-component of the electric field is given by $E = m\varphi'/q$. The potential φ is chosen to vanish ahead of the laser pulse and, alongside φ', is required to be continuous across discontinuities in a.

It is straightforward to show (32) and (55) are equivalent by rearranging (55) to give

$$1+\varphi = \sqrt{1+a^2}\,\frac{\omega_p^2+\varphi'' - v^2\varphi''}{\sqrt{\left(\omega_p^2+\varphi''\right)^2 - v^2\varphi''^2}}. \tag{56}$$

Differentiating (56) with respect to ζ and noting $\varphi' = \omega_p^2\psi$ (since $E = qn_{\text{ion}}\psi = m\varphi'/q$ and $\omega_p = \sqrt{q^2 n_{\text{ion}}/m}$) immediately gives (32). Furthermore, inspection of (56) shows that the continuity of φ across any discontinuity in a leads to the jump conditions on ψ' developed in sections 3.1–3.3.

Equation (55) is readily amenable to analysis in the limit $\gamma \to \infty$ [2, 19]. Substituting $v = \sqrt{1-\gamma^{-2}}$ in (55) and letting $\gamma \to \infty$ yields

$$\varphi'' = \frac{\omega_p^2}{2}\left(\frac{1+a^2}{(1+\varphi)^2} - 1\right). \tag{57}$$

The solutions to (57), when a is constant, can be readily expressed in terms of elliptic integrals [19]. However, for present purposes, we only require the first integral of (57). The potential $\varphi_{(1)}$ inside the pulse satisfies

$$\check{\mathcal{E}}_{(1)} = \frac{1}{2}\varphi_{(1)}'^2 + \frac{\omega_p^2}{2}\left(\frac{1+a_0^2}{1+\varphi_{(1)}} + \varphi_{(1)}\right) \tag{58}$$

where $\check{\mathcal{E}}_{(1)}$ is constant, with the caron distinguishing quantities from those associated with (32). The constant of integration $\check{\mathcal{E}}_{(1)}$ is determined by noting $\varphi_{(1)}$ and $\varphi'_{(1)}$ vanish at the front of the pulse (since the potential $\varphi_{(0)}$, and its derivative, ahead of the pulse vanish). This choice yields a_0^2 for the maximum of $\varphi_{(1)}$. Likewise, results for optimal-length pulse are obtained by fixing the constant of integration

$$\check{\mathcal{E}}_{(2)} = \frac{1}{2}\varphi_{(2)}'^2 + \frac{\omega_p^2}{2}\left(\frac{1}{1+\varphi_{(2)}} + \varphi_{(2)}\right) \tag{59}$$

associated with the potential $\varphi_{(2)}$ behind the pulse by equating $\varphi_{(2)}$ and $\varphi_{(1)}$, and their first derivatives, at the back of the pulse. The electric field component E vanishes at the back of an optimal-length pulse, and so $\varphi'_{(2)}$ and $\varphi'_{(1)}$ both vanish at the back of the pulse. The potential is maximal at the back of the pulse; hence $\varphi_{(1)}$ (and thus $\varphi_{(2)}$) equals a_0^2 there. It follows that the amplitude $|\check{E}_{(2)\max}|$ of the z-component of the electric field of the wake satisfies

$$|\check{E}_{(2)\max}| = \frac{m\omega_p}{|q|}\,\frac{a_0^2}{\sqrt{1+a_0^2}}. \tag{60}$$

Although (60) is valid for all a_0, unlike (49) it is only valid in the limit $\gamma \to \infty$. On the other hand, (49) is valid for all subluminal v but, unlike (60), it is only valid for the strongest possible periodic wake (i.e. the wake produced when $a_0 = a_{0c}$). The amplitude of the electric field of the strongest possible periodic wake is given by the Akhiezer–Polovin limit [28]

$$|E_{\text{AP}}| = \frac{m\omega_p}{|q|}\sqrt{2(\gamma-1)}. \tag{61}$$

Clearly, $|\check{E}_{(2)\max}|/|E_{\mathrm{AP}}| \to 1$ as $\gamma \to \infty$ if $a_0/\sqrt{2\gamma} \to 1$. Inspection of (49) shows that the critical value of a_0 behaves as required.

The Lorentz factor γ for laser-driven plasma waves is typically between 10 and 100 [2]. Setting $\gamma = 10$ in (49) yields $a_{0\mathrm{c}} = 4.2$ (1 decimal place), whereas the estimate $a_{0\mathrm{c}} \approx \sqrt{2\gamma}$ inferred from (60) and (61) yields $a_{0\mathrm{c}} \approx 4.5$ (1 decimal place). A similar calculation when $\gamma = 100$ yields essentially the same value, 14.1 (1 decimal place), for $a_{0\mathrm{c}}$ using either approach. From a practical perspective, the dimensionless laser amplitude is often substantially below $a_{0\mathrm{c}}$ (e.g. $a_0 = 2$ when $\gamma = 10$ [2]), so the estimate $a_{0\mathrm{c}} \approx \sqrt{2\gamma}$ is sufficient in most physical applications. However, if greater accuracy is required then (49) is valid to any precision. In particular, as noted at the start of this section, numerical investigation of the exact result (49) reveals $a_{0\mathrm{c}} \approx \sqrt{2(\gamma-1)}$ is remarkably accurate (to within 3.2%) for all subluminal v.

4. Conclusion

The laser wakefield accelerator paradigm is a key aspect of the development of new particle accelerator technology. Although state-of-the-art three-dimensional particle-in-cell codes underpin research in this area, reduced models and analytical results remain useful for making preliminary estimates. With this in mind, we have developed a relativistically covariant, non-linear, scalar field theory from a $2+2$ decomposition of the cold fluid description of a laser-driven plasma. We have shown that if the laser pulse is prescribed, then the resulting theory naturally yields an upper bound on the dimensionless amplitude a_0 of a circularly polarised laser pulse with a top-hat envelope whose duration is one-half of the period of the wake. We find that the expression for the critical value of a_0 agrees with the quantity $\sqrt{2(\gamma-1)}$ to within 3.2% accuracy, where γ is the Lorentz factor of the speed v of the laser-driven wake. It follows that the ratio of the critical values of the electric fields of the laser pulse and the plasma wake essentially agrees with the ratio of the frequencies of the laser and the plasma. Conventional analytical approaches tend to make use of approximations valid in the limit as v tends to c, and the asymptotic behaviour of our expression for the critical dimensionless amplitude agrees with those analyses.

Data availability statement

All data that support the findings of this study are included within the article (and any supplementary files).

Acknowledgments

We thank the referees for their useful comments and suggestions. This work was supported by the Lancaster University Faculty of Science and Technology. All of the results can be fully reproduced using the methods described in the paper.

Appendix

Equation (49) can be directly obtained from (47) and (48) as follows. Introducing the variables

$$\xi = \frac{v\psi'^{+}_{(1\cap 2)}}{1+\psi'^{+}_{(1\cap 2)}}, \qquad r = \sqrt{1+a_{0\mathrm{c}}^2} \tag{A.1}$$

allows (47) and (48) to be written as

$$\gamma\left(1+v^2\right) = \frac{r(1-v\xi)}{\sqrt{1-\xi^2}}, \tag{A.2}$$

$$\eta = \frac{r}{\sqrt{1-\xi^2}} \tag{A.3}$$

respectively, where η is given in (51). Combining (A.2) and (A.3) immediately gives

$$\gamma\left(1+v^2\right) = \eta(1-v\xi) \tag{A.4}$$

whilst solving (A.3) for ξ yields

$$\xi = \pm\sqrt{1-\frac{r^2}{\eta^2}}. \tag{A.5}$$

Hence, substituting ξ in (A.4) using (A.5) gives

$$\gamma\left(1+v^2\right) = \eta \mp v\sqrt{\eta^2-r^2}. \tag{A.6}$$

However, making use of $\gamma = 1/\sqrt{1-v^2}$ allows

$$\eta^2 - r^2 = \gamma^2\left(\sqrt{\gamma^2-r^2}-\gamma v\right)^2 \tag{A.7}$$

to be obtained from (51); thus

$$\sqrt{\eta^2-r^2} = \pm\gamma\left(\sqrt{\gamma^2-r^2}-\gamma v\right). \tag{A.8}$$

Hence, substituting η and $\sqrt{\eta^2-r^2}$ in (A.6) using (51) and (A.8), respectively, leads to

$$\gamma\left(1+v^2\right) = \gamma^2 - \gamma v\sqrt{\gamma^2-r^2} \pm \gamma v\left(\sqrt{\gamma^2-r^2}-\gamma v\right). \tag{A.9}$$

However, the upper sign in (A.9) must be discarded because it yields $\gamma(1+v^2) = 1$, whose solution is $v = 0$. The lower sign gives

$$\gamma\left(1+v^2\right) = \gamma^2\left(1+v^2\right) - 2\gamma v\sqrt{\gamma^2-1-a_{0c}^2} \tag{A.10}$$

where r has been substituted using (A.1). Solving (A.10) for a_{0c}^2, and making use of $\gamma = 1/\sqrt{1-v^2}$, reveals (49).

ORCID iDs

Mark Aleksiejuk https://orcid.org/0000-0001-7764-366X
David A Burton https://orcid.org/0000-0003-1303-0877

References

[1] Tajima T and Dawson J M 1979 *Phys. Rev. Lett.* **43** 267–70
[2] Esarey E, Schroeder C B and Leemans W P 2009 *Rev. Mod. Phys.* **81** 1229–84
[3] Hooker S M 2013 *Nat. Photon.* **7** 775–82
[4] Albert F 2023 *Phys. Plasmas* **30** 050902
[5] Mangles S P D *et al* 2004 *Nature* **431** 535–8
[6] Geddes C G R , Toth C, van Tilborg J, Esarey E, Schroeder C B, Bruhwiler D, Nieter C, Cary J and Leemans W P 2004 *Nature* **431** 538–41
[7] Faure J , Glinec Y, Pukhov A, Kiselev S, Gordienko S, Lefebvre E, Rousseau J-P, Burgy F and Malka V 2004 *Nature* **431** 541–4
[8] Gonsalves A J *et al* 2019 *Phys. Rev. Lett.* **122** 084801
[9] Schlenvoigt H-P *et al* 2008 *Nat. Phys.* **4** 130–3
[10] Albert F *et al* 2014 *Plasma Phys. Control. Fusion* **56** 084015
[11] Albert F and Thomas A G R 2016 *Plasma Phys. Control. Fusion* **58** 103001
[12] Assmann R W *et al* 2020 *Eur. Phys. J. Spec. Top.* **229** 3675–4284
[13] Schroeder C B *et al* 2023 *J. Instrum.* **18** T06001
[14] Albert F *et al* 2021 *New J. Phys.* **23** 031101
[15] Fonseca R A *et al* 2002 *Computational Science - ICCS 2002* (*Lecture Notes in Computer Science* vol 2331) ed P M A Sloot, A G Hoekstra, C J K Tan and J J Dongarra pp 342–51
[16] Arber T D *et al* 2015 *Plasma Phys. Control. Fusion* **57** 113001
[17] Pukhov A and Meyer-Ter-Vehn J 2002 *Appl. Phys.* B **74** 355
[18] Lu W, Tzoufras M, Joshi C, Tsung F S, Mori W B, Vieira J, Fonseca R A and Silva L O 2007 *Phys. Rev. Spec. Top. Accel. Beams* **10** 061301
[19] Bulanov S V , Esirkepov T Z, Hayashi Y, Kiriyama H, Koga J K, Kotaki H, Mori M and Kando M 2016 *J. Plasma Phys.* **82** 905820308
[20] Sandberg R T and Thomas A G R 2023 *Phys. Rev. Lett.* **130** 085001
[21] Burton D A and Noble A 2018 *New J. Phys.* **20** 033022
[22] Trines R M G M 2009 *Phys. Rev.* E **79** 056406
[23] Burton D A and Noble A 2024 *A Geometric Approach to Physics* (CRC Press)
[24] Frankel T 2011 *The Geometry of Physics: an Introduction* (Cambridge University Press)
[25] Dawson J 1962 *Phys. Fluids* **5** 445–59
[26] Fiore G, De Nicola S, Akhter T, Fedele R and Jovanović D 2023 *Physica* D **454** 133878
[27] Fiore G 2018 *J. Phys. A: Math. Theor.* **51** 085203
[28] Akhiezer A I and Polovin R V 1956 *Sov. Phys - JETP* **3** 696–704